AGU PUBLICATIONS

JGR Earth Surface

Supporting Information for

Controls on Physical and Chemical Denudation in a Mixed Siliciclastic-Carbonate Orogen

E. D. Erlanger[1], J. K. C. Rugenstein[2], A. Bufe[1], V. Picotti[3], and S. D. Willett[3]

[1]GFZ, Telegrafenberg, Potsdam, Germany

[2]Department of Geosciences, Colorado State University, Fort Collins, CO 80521, USA

[3]Department of Earth Science, ETH Zürich, Zürich, Switzerland

Contents of this file

Introduction

Text in the supporting information refers to methods used to perform the secondary calcite correction to our dataset. Tables in the supporting information provide sample information, solute concentrations, or calculated metrics (e.g. saturation index) as a reference for figures included in the main text. Figures in the supporting information illustrate either aspects or justifications for the methods employed in this paper (Figures S2, S3, and S5), or provide support for explanations given in the text (S1,S4, S6). We note that none of the figures presented here are necessary for comprehending the main text.

Evaporite Weathering (Text S1)

In the absence of evaporite deposits, the total amounts of Ca^{2+} and Mg^{2+} in water samples reflect weathering of both silicates and carbonates. However, evaporites such as gypsum ($CaSO_4$) may represent another substantial source of dissolved, riverine Ca^{2+} (Meybeck, 1987). In carbonate catchments, the expected stoichiometric ratio of (Ca + Mg)/HCO_3 is 0.5 in pristine water (Sarin et al., 1989; Perrin et al., 2008). In the absence of evaporite deposits, calculated ratios along the Brahmaputra River are 1.09 ± 0.1 (Sarin et al., 1989), and between 1–2 for small catchments in France that were cultivated with nitrogen fertilizers (Perrin et al., 2008). The average (Ca + Mg)/HCO_3 ratio and 2σ errors for our river samples is 1.21 ± 0.32 (R^2 = 0.74), a value that indicates negligible Ca- and Mg-bearing evaporite sources. High concentrations of SO_4^{2-}, Na^+, and Ca^{2+} were found in three of the studied catchments (3, 5, and 15). These rivers fell outside the average ratios of (Ca + Mg)/HCO_3 for all other catchments, consistent with observations of evaporite sources (halite and gypsum) in catchments 3 and 15 (Cortecci et al., 2008; Chiesi et al., 2010; Boschetti et al., 2011), and were therefore excluded from the weathering flux calculations (Figure S2).

Secondary Precipitation Corrections (Text S2)

Secondary precipitation of calcite from supersaturated waters, and the consequent enrichment of Sr^{2+} in the remaining solution, has been observed in the Himalaya and in Taiwan (Bickle et al., 2015; Emberson, Galy, & Hovius, 2018; Jacobson, Blum, & Walter, 2002). This enrichment can be estimated by calculating the deviation of solute samples from a mixing line between a silicate and carbonate endmember in Na/Ca and Sr*1000/Ca space.

To estimate the endmember composition of local bedrock, we use published geochemical data of bedrock samples in the Northern Apennines (Bracciali et al., 2007; Dinelli et al., 1999). Carbonates are assumed to have negligible Na^+, so the carbonate endmember is defined as the inferred Sr/Ca content when Na/Ca equals zero (Bickle et al., 2015). We estimate the silicate endmember for each lithology using major ions and the trace element composition of sandstones from the Tertiary Foredeep Units (Dinelli et al., 1999), and from various lithologies in the Ligurian Units (Bracciali et al., 2007). We use a linear regression through all data points as the endmember mixing line for each lithology (Figure S4). For the Tertiary Foredeep deposits, we differentiate between the Marnoso Arenacea Unit and the Macigno-Cervarola Units. We additionally differentiate between the Internal and External Ligurian Units, as the bedrock composition is sufficiently different between the two units (Figure S4, c-d) to warrant treating them separately (Bracciali et al., 2007). To constrain the endmember mixing line for the External Ligurian Unit, we used chemical data of the solids from the exposed formation, or, where available, local data from sand within the specific catchment (Bracciali et al., 2007). We have no constraints on the bedrock composition of the Epi-Ligurian Unit. However, in most cases the Epi-Ligurian Unit represents deposition in satellite basins that were coeval with and coupled with the deposition of the Tertiary Foredeep Units (Ricci Lucchi, 1986), so we expect that the composition of these units should be similar.

Samples were corrected for secondary calcite precipitation using a partition coefficient of k = 0.05. Previous studies suggest that the acceptable range of values for k is 0.02-0.2 (Tesoriero and Pankow, 1996; Gabitov and Watson, 2006; Nehrke et al., 2007). We also performed the correction for secondary calcite precipitation for two endmember scenarios (k = 0.02 and k = 0.2) to assess the variability in the adjusted [Ca^{2+}] concentrations (Figure S5). Using a lower k value results in a smaller correction to [Ca^{2+}], so the value used for our correction (k = 0.05) could be interpreted as a minimum; however, regardless of the k value used, the resulting correction to the original [Ca^{2+}] concentrations is substantial.

We corrected all supersaturated water samples for secondary calcite precipitation, even those that drain mixed lithologies (catchments 8–9 and 17–18) (Table S3). A subset of water samples that predominantly drain a single lithology were used to constrain the overall water chemistry for each lithology. For example, we corrected catchments 8-9 with the External Ligurian bedrock mixing line (Table S3), because over half of the catchment is covered by the External Ligurian Unit.

For catchment 17, the External Ligurian Unit covers 55% the catchment area, although we observe no offset between the water sample ratios and the External Ligurian bedrock mixing line, suggesting that no significant secondary calcite precipitation occurs in these catchments. However, this river has highly oversaturated waters (SI = 0.9), so we are confident that secondary calcite precipitation is in fact occurring along this river. We thus correct for secondary calcite in this catchment using the bedrock mixing line for the Tertiary Foredeep Units (Cervarola and Epi-Ligurian Units) (Figure 1a). These units comprise the remaining 45% of the catchment area, and we observe an offset between the water sample ratios and bedrock mixing line, as expected for oversaturated samples.

We did not correct the [Ca^{2+}] in undersaturated and saturated samples, because no secondary calcite precipitation is expected, which is consistent with the observation that the water chemistry could not be differentiated from the bedrock geochemical compositions for these samples.

Global Denudation and Weathering Flux Dataset Calculations (Text S3).

A variety of methods have been employed to calculate the associated denudation and physical erosion fluxes for the global dataset. Most estimates of physical erosion in these data are derived from stream sediment fluxes (Hodson et al., 2000; Millot et al., 2002; Picouet et al., 2002; Hosein et al., 2004; West et al., 2005). A small subset of studies have calculated denudation and physical erosion fluxes from detrital cosmogenic nuclides measured in river sediments (Galy and France-Lanord, 2001; West et al., 2005). In turn, chemical weathering fluxes are calculated using either annual average element budgets or spot chemistry measurements combined with annual discharge.

We compare our data to studies that also calculated chemical weathering fluxes either from oxide concentrations of Ca^{2+}, Mg^{2+}, K^{+}, Na^{+}, and Si or from cation concentrations. Most global data points were extracted from West et al. (2005), from which we estimate weathering fluxes using the "Total Cation Denudation Rates fluxes" (TCDR), combined with weathering estimates of Si from SiO_2 fluxes. We also recalculated weathering fluxes for datapoints from the Andes (Gaillardet et al., 1997) using the methods employed in this paper, and corrected the initial concentrations for atmospheric Cl^{-} inputs using the weighted average composition of rainwater in the Amazon basin (8.31 μmol/L) calculated by Gaillardet al. (1997).

References

Bickle, M.J., Tipper, E., Galy, A., Chapman, H., and Harris, N., 2015, On discrimination between carbonate and silicate inputs to Himalayan rivers: American Journal of Science, v. 315, p. 120–166, doi:10.2475/02.2015.02.

Boschetti, T., Cortecci, G., Toscani, L., and Iacumin, P., 2011, Sulfur and oxygen isotope compositions of Upper Triassic sulfates from northern Apennines (Italy): Paleogeographic and hydrogeochemical implications: Geologica Acta, v. 9, p. 129–147, doi:10.1344/105.000001690.

Bracciali, L., Marroni, M., Pandolfi, L., Rocchi, S., Arribas, J., Critelli, S., and Johnsson, M.J., 2007, Geochemistry and petrography of Western Tethys Cretaceous sedimentary covers (Corsica and Northern Apennines): from source areas to configuration of margins: Special Paper of the Geological Society of America, v. 420, p. 73.

Chiesi, M., Waele, J. De, and Forti, P., 2010, Origin and evolution of a salty gypsum / anhydrite karst spring : the case of Poiano (Northern Apennines , Italy): , p. 1111–1124, doi:10.1007/s10040-010-0576-2.

Cortecci, G., Dinelli, E., Boschetti, T., Arbizzani, P., Pompilio, L., and Mussi, M., 2008, The

Serchio River catchment, northern Tuscany: Geochemistry of stream waters and sediments, and isotopic composition of dissolved sulfate: Applied Geochemistry, v. 23, p. 1513–1543, doi:10.1016/j.apgeochem.2007.12.031.

Dinelli, E., Lucchini, F., Mordenti, A., and Paganelli, L., 1999, Geochemistry of Oligocene-Miocene sandstones of the northern Apennines (Italy) and evolution of chemical features in relation to provenance changes: Sedimentary Geology, v. 127, p. 193–207, doi:10.1016/S0037-0738(99)00049-4.

Emberson, R., Galy, A., and Hovius, N., 2018, Weathering of Reactive Mineral Phases in Landslides Acts as a Source of Carbon Dioxide in Mountain Belts: Journal of Geophysical Research: Earth Surface, p. 2695–2713, doi:10.1029/2018JF004672.

Gabitov, R.I., and Watson, E.B., 2006, Partitioning of strontium between calcite and fluid: Geochemistry, Geophysics, Geosystems, v. 7.

Gaillardet, J., Dupre, B., Allegre, C.J., and Négrel, P., 1997, Chemical and physical denudation in the Amazon River Basin: Chemical geology, v. 142, p. 141–173.

Galy, A., and France-Lanord, C., 2001, Higher erosion rates in the Himalaya: Geochemical constraints on riverine fluxes: Geology, v. 29, p. 23–26.

Garzanti, E., Canclini, S., Moretti Foggia, F., and Petrella, N., 2002, Unraveling magmatic and orogenic provenances in modern sands: the back-arc side of the Apennine thrust-belt (Italy): Journal of Sedimentary Research, v. 72, p. 2–17, doi:10.1306/051801720002.

Garzanti, E., Scutellà, M., and Vidimari, C., 1998, Provenance from ophiolites and oceanic allochtons: Modern beach and river sands from Liguria and the northern Apennines (Italy): Ofioliti, v. 23, p. 65–82, doi:10.4454/ofioliti.v23i2.2.

Hodson, A., Tranter, M., and Vatne, G., 2000, Contemporary rates of chemical denudation and atmospheric CO2 sequestration in glacier basins: an Arctic perspective: Earth Surface Processes and Landforms, v. 25, p. 1447–1471.

Hosein, R., Arn, K., Steinmann, P., and Adatte, T., 2004, Carbonate and silicate weathering in two presently glaciated, crystalline catchments in the Swiss Alps: Geochimica et Cosmochimica Acta, v. 68, p. 1021–1033.

Jacobson, A.D., Blum, J.D., and Walter, L.M., 2002, Reconciling the elemental and Sr isotope composition of Himalayan weathering fluxes: Insights from the carbonate geochemistry of stream waters: Geochimica et Cosmochimica Acta, v. 66, p. 3417–3429, doi:10.1016/S0016-7037(02)00951-1.

Meybeck, M., 1987, Global chemical weathering of surficial rocks estimated from river dissolved loads: American journal of science, v. 287, p. 401–428.

Millot, R., Gaillardet, J., Dupré, B., and Allègre, C.J., 2002, The global control of silicate weathering rates and the coupling with physical erosion: New insights from rivers of the Canadian Shield: Earth and Planetary Science Letters, v. 196, p. 83–98, doi:10.1016/S0012-821X(01)00599-4.

Nehrke, G., Reichart, G.-J., Van Cappellen, P., Meile, C., and Bijma, J., 2007, Dependence of calcite growth rate and Sr partitioning on solution stoichiometry: non-Kossel crystal growth: Geochimica et Cosmochimica Acta, v. 71, p. 2240–2249.

Perrin, A.S., Probst, A., and Probst, J.L., 2008, Impact of nitrogenous fertilizers on carbonate dissolution in small agricultural catchments: Implications for weathering CO2 uptake at regional and global scales: Geochimica et Cosmochimica Acta, v. 72, p. 3105–3123, doi:10.1016/j.gca.2008.04.011.

Picouet, C., Dupré, B., Orange, D., and Valladon, M., 2002, Major and trace element geochemistry in the upper Niger river (Mali): physical and chemical weathering rates and CO2 consumption: Chemical Geology, v. 185, p. 93–124.

Ricci Lucchi, F., 1986, The Oligocene to Recent Foreland Basins of the Northern Apennines, *in* Allen, A. and Homewood, P. eds., Foreland Basins, Blackwell Scientific Oxford, Wiley Online Books, p. 105–139, doi:doi:10.1002/9781444303810.ch6.

Sarin, M.M., Krishnaswami, S., Dilli, K., Somayajulu, B.L.K., and Moore, W.S., 1989, Major ion chemistry of the Ganga-Brahmaputra river system: Weathering processes and fluxes to the Bay of Bengal: Geochimica et Cosmochimica Acta, v. 53, p. 997–1009, doi:10.1016/0016-7037(89)90205-6.

Tesoriero, A.J., and Pankow, J.F., 1996, Solid solution partitioning of Sr2+, Ba2+, and Cd2+ to calcite: Geochimica et Cosmochimica Acta, v. 60, p. 1053–1063.

West, A.J., Galy, A., and Bickle, M., 2005, Tectonic and climatic controls on silicate weathering: Earth and Planetary Science Letters, v. 235, p. 211–228, doi:10.1016/j.epsl.2005.03.020.

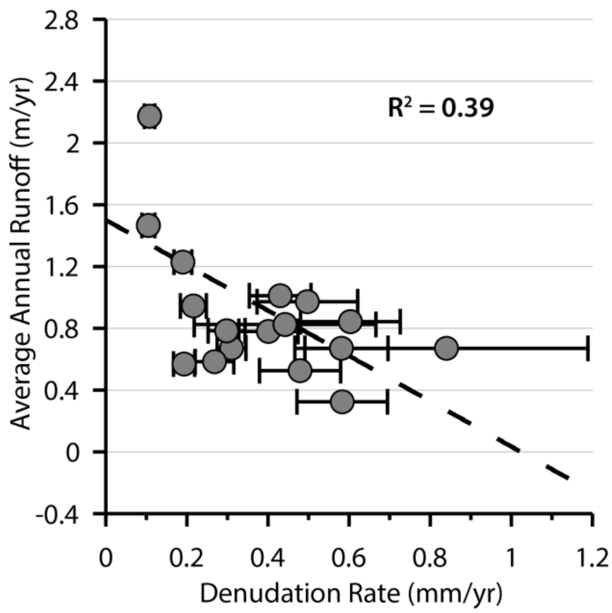

Figure S1. *Denudation rates plotted against annual runoff estimates averaged over the last five available years of data.*

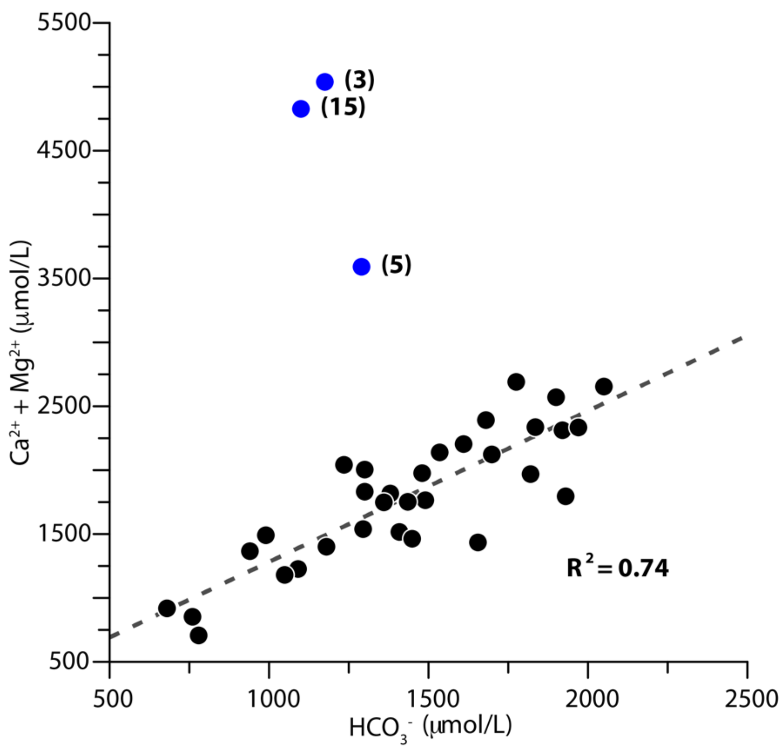

Figure S2. *Plot of HCO_3 against Ca + Mg. Linear regression (dashed line) and R^2 statistic apply only to black data points. Outlier data points are illustrated as blue circles; numbers correspond to river numbers shown in Figure 1a.*

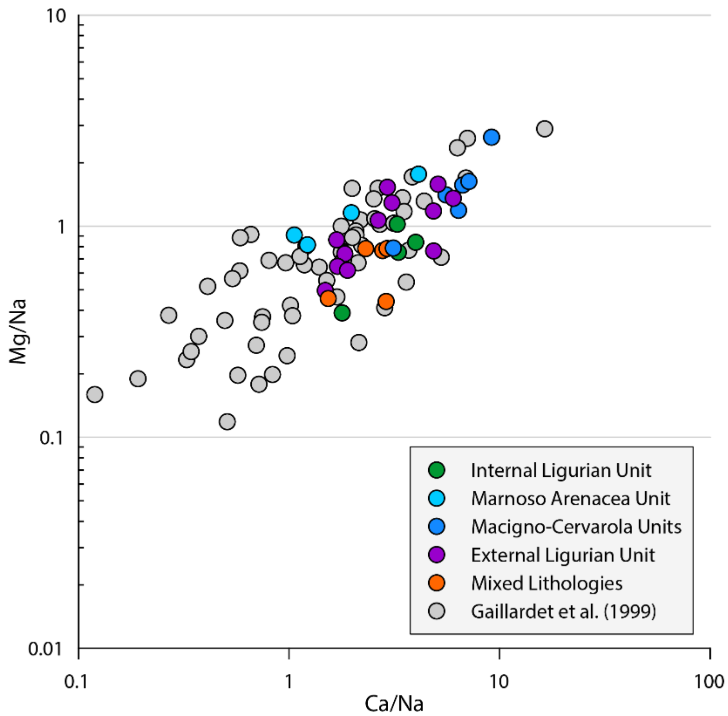

Figure S3. *Mixing diagram comparing ratios of Ca/Na and Mg/Na for different lithologies in the Northern Apennines (colored circles) with Gaillardet et al. (1999) global dataset (gray circles).*

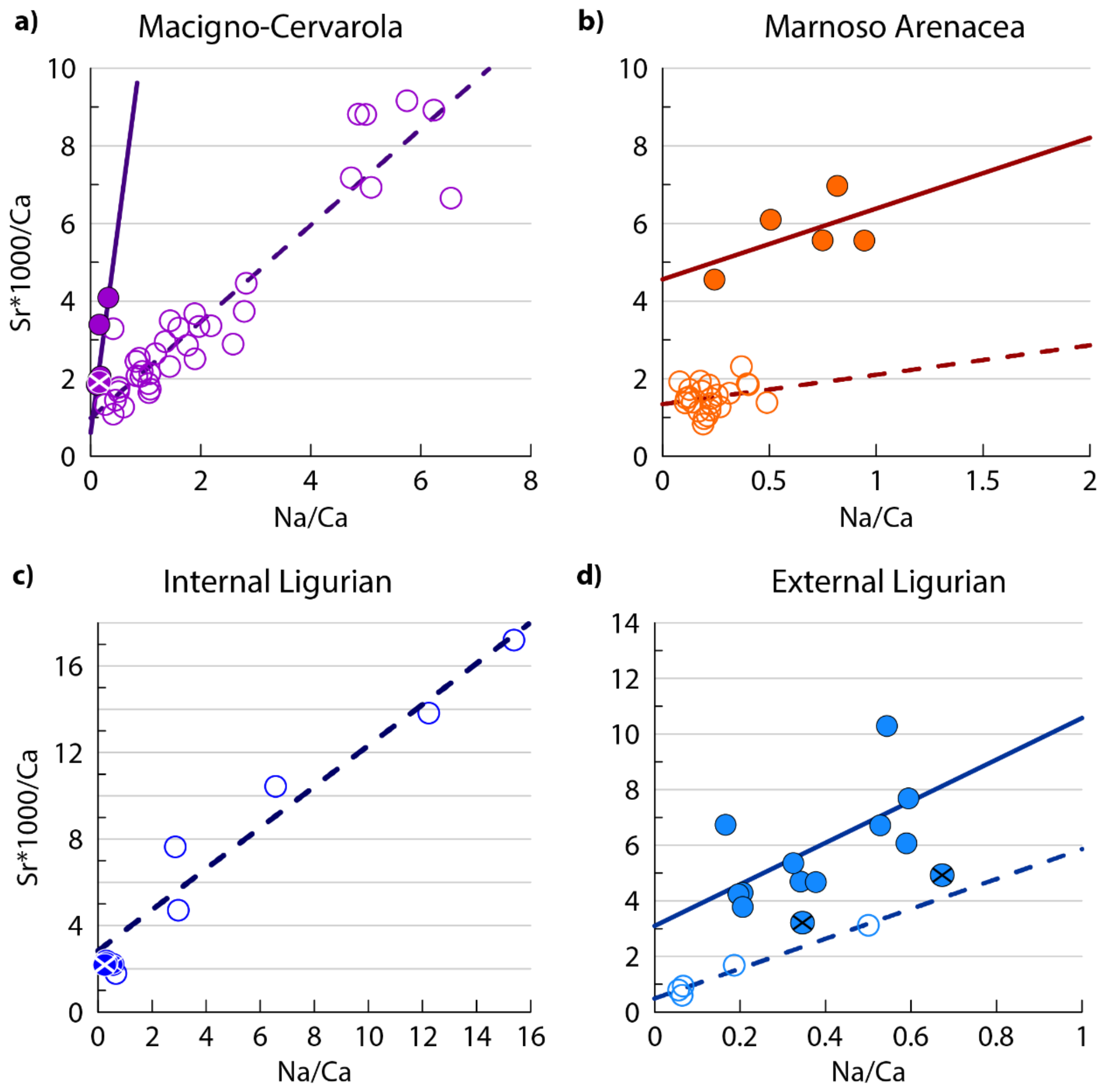

Figure S4. *a-d) Ratios of Na/Ca plotted against Sr*1000/Ca for the primary lithologic units in the study area. Open circles and dashed regression lines represent bedrock data for each unit from Dinelli et al (1999) for the a) Macigno-Cervarola and b) Marnoso Arenacea Units and from Bracciali et al. (2007) for the c) Internal Ligurian Unit and d) External Ligurian Unit. Closed circles represent catchments analyzed in this study, which were categorized based on the dominant lithologic unit draining the catchment. Circles with an "x" through the center represent samples that were not corrected for secondary calcite precipitation.*

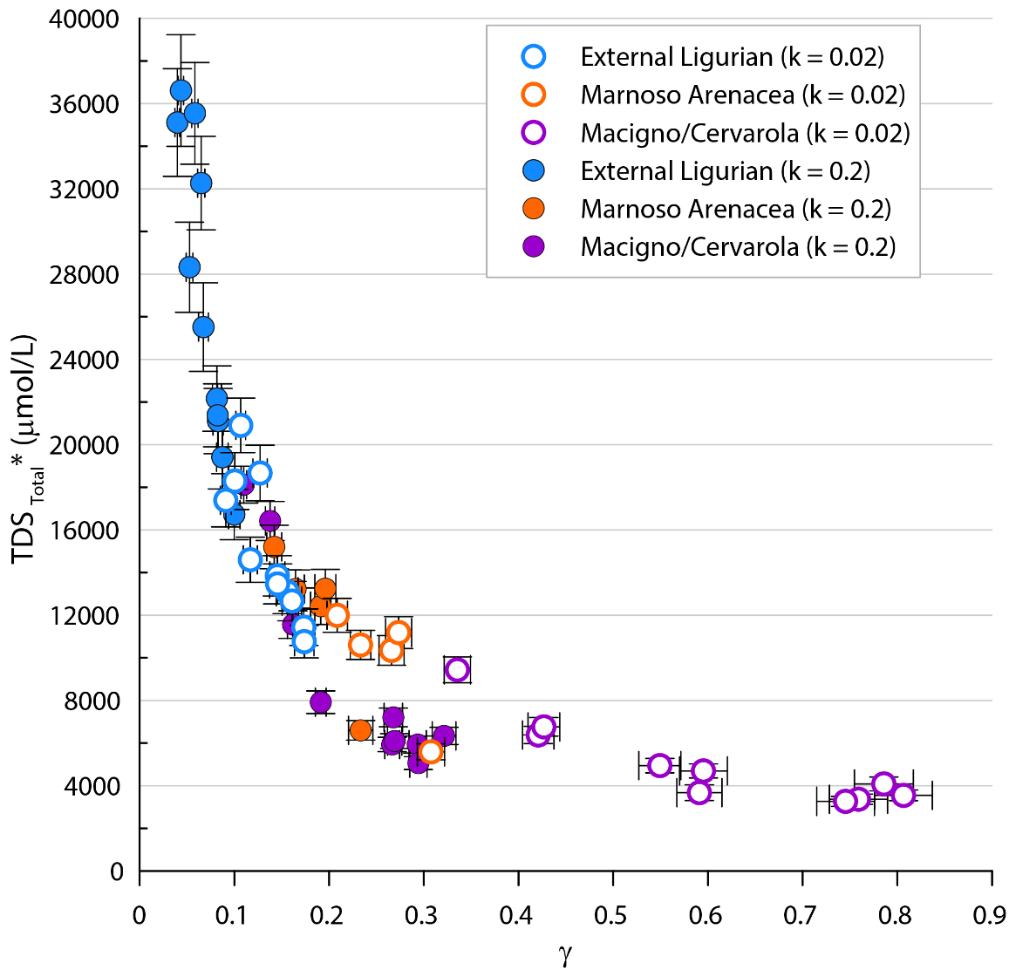

Figure S5. *Endmember corrections for secondary calcite precipitations using k = 0.02 (outlined circles) and k = 0.2 (filled circles). Internal Ligurian Unit is neglected as samples draining this unit were not corrected for secondary calcite precipitation.*

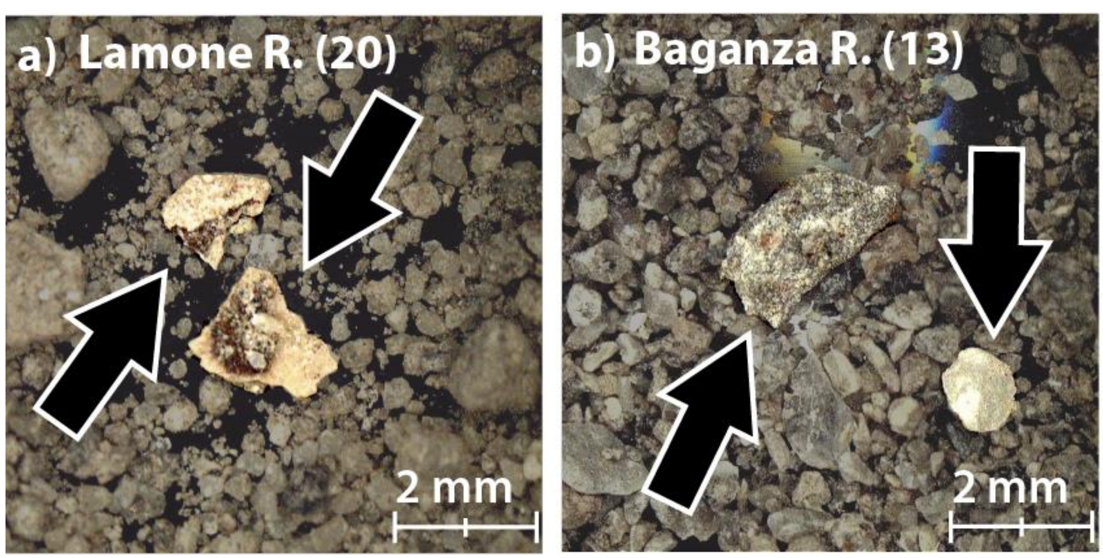

Figure S6. *Examples of carbonate grains from a) the Lamone River (River No. 20) and b) the Baganza River (River No. 13). Grains of interest are highlighted relative to the background and are indicated with arrows in each figure. a) Example of a secondary calcite grain comprised of organic matter (dark material at center of both pieces) surrounded by a carbonate crust. b) Examples of primary carbonate grains in the Baganza River. The upper-left grain is comprised of sparry micrite and the lower-right grain is a single-grain calcite.*

	River/Location	Latitude	Longitude	Basin Area (km^2)	% Carbonate Sand (250-500 μm)	L_c grain counts	Avg Size of L_c grains (μm)
1	Bisenzio	43.9278°	11.1258°	149	28	NA	NA
2	Lima	43.9993°	10.5539°	317	20	NA	NA
3	Serchio at Piaggone	43.9299°	10.5060°	1160	24	33†	NA
4	Serchio at Filicaia	44.1360°	10.3762°	252	N.A.	NA	NA
5	Magra	44.1869°	9.9256°	947	25	20†	NA
6	Vara	44.1899°	9.8578°	555	18	6*	540*
7	Entella	44.3509°	9.3619°	297	17	7*	620*
8	Scrivia	44.7194°	8.86056°	615	57	36*	310*
9	Staffora	44.8930°	9.0569°	264	49	55*	300*
10	Trebbia	44.9089°	9.5893°	918	60	45*	400*
11	Nure	44.8816°	9.6532°	343	67	57*	310*
12	Taro	44.6976°	10.0934°	1250	63	43*	570*
13	Baganza	44.6842°	10.2130°	153	76	70*	310*
14	Parma	44.5688°	10.2370°	264	71	74*	140*
15	Enza	44.6267°	10.4133°	481	60	53*	235*
16	Secchia	44.5431°	10.767	1010	47	40*	190*
17	Panaro	44.4196°	10.925	680	38	51*	310*
18	Reno	44.3923°	11.257	990	36	28*	580*
19	Senio at Palazzuolo	44.2266°	11.632	136	25	NA	NA
20	Lamone at Biforco	44.0651°	11.601	179	21	NA	NA
21	Montone at Davadola	44.1201°	11.885	190	42	NA	NA

* Data from Garzanti et al. (1998) Ligurian Rivers (1-7) were sampled along the coastline and Adriatic Rivers (8-21) were sampled at the mountain front.

† Data from Garzanti et al. (2002). Values refer to estimates for the Massa Carrara Unit that is drained by the Magra River (5) or the Pisa Province that is drained by the Serchio River (3).

Table S1. *Sampling locations, basin area, and % catchment-averaged percent carbonate sand from this study. Lithic carbonate (Lc) point counts and average grain size for each catchment (where available) from Garzanti et al. (1998, 2002).*

Catchment Number	Catchment Name	Locality	Sample Number	Latitude	Longitude	Collection Date (dd.mm.yy)	Elevation (m)	T (°C)	pH	Ca^{2+}	K^{+}	Mg^{2+}	Na^{+}	Sr^{2+}	Si	Cl^{-}	SO_4^{2-}	HCO_3^{-}	NO_3^{-}
1	Bisenzio	Vaiano	1	43.926°	11.127°	15.07.18	118	26.0	8.84	2120.3	80.2	562.7	4483.1	5.7	133.3	1540.6	797.2	1775.0	65.1
2	Lima	Cutigliano	1	44.099°	10.752°	04.05.17	594	7.9	7.80	596.2	10.2	102.9	93.4	1.1	73.7	42.5	54.5	779.3	5.0
2	Lima	Borgo a Mozzano	1	43.999°	10.554°	15.07.18	102	24.0	8.64	1184.4	22.5	298.6	378.8	4.8	76.4	235.3	407.6	990.0	15.9
3	Serchio	Piaggione	1	43.935°	10.506°	15.07.18	51	21.2	8.14	3713.3	47.4	1317.4	1540.6	31.4	133.9	1053.1	3333.8	1175.0	43.5
4	Serchio	Filicaia	1	44.137°	10.374°	15.07.18	318	21.3	8.74	1682.8	25.2	313.9	263.7	5.7	105.4	116.2	533.9	1300.0	18.2
5	Magra	Aulla	1	44.187°	9.926°	20.03.18	55	9.9	8.19	1178.7	22.3	179.5	407.7	3.8	117.8	408.5	219.2	940.0	0.0
5	Magra	Aulla	2	44.187°	9.926°	15.07.18	28	22.5	8.42	3058.3	50.3	525.4	3314.2	14.4	74.1	2381.8	1327.3	1290.0	17.8
6	Vara	Piana Battolla	1	44.192°	9.858°	20.03.18	37	9.6	7.70	688.1	17.7	156.8	208.2	1.6	136.6	186.9	95.5	760.0	0.0
6	Vara	Piana Battolla	2	44.190°	9.858°	15.07.18	44	24.8	8.51	1165.6	25.0	365.4	357.2	2.8	119.3	179.5	132.4	1295.0	10.6
7	Entella	Carasco	1	44.351°	9.362°	20.03.18	12	9.4	8.03	752.6	13.0	158.2	188.5	1.6	96.2	185.8	78.9	680.0	0.0
7	Entella	Carasco	2	44.351°	9.362°	15.07.18	12	20.6	8.11	1171.9	27.7	254.8	655.9	2.6	117.0	305.5	98.6	1655.0	33.4
8	Scrivia	Serravalle Scrivia	1	44.719°	8.860°	18.03.18	208	7.8	8.35	1545.1	24.1	242.7	317.9	6.6	89.8	270.3	195.5	1930.0	0.0
9	Staffora	Godiasco	1	44.893°	9.057°	15.07.18	191	27.4	8.26	1409.5	70.5	721.9	837.2	10.8	254.4	265.2	419.9	1535.0	9.1
10	Trebbia	Rivergaro	1	44.908°	9.590°	22.03.18	131	4.5	8.37	1399.9	20.9	340.7	288.6	5.3	103.7	240.1	207.8	1360.0	0.0
10	Trebbia	Rivergaro	2	44.909°	9.589°	15.07.18	131	23.7	7.77	1356.6	37.4	452.9	912.7	6.7	150.2	620.3	228.1	1380.0	38.3
11	Nure	Vigolzone	1	44.882°	9.653°	21.03.18	178	7.8	8.23	1805.8	36.9	757.1	586.1	9.7	133.2	153.6	744.9	1900.0	0.0
11	Nure	Lugherzano	2	44.828°	9.617°	15.07.18	258	24.8	8.35	1442.9	44.4	753.7	492.5	6.8	199.9	114.1	294.1	1610.0	34.1
12	Taro	Ramiola	1	44.698°	10.093°	21.03.18	127	5.5	8.46	1496.9	36.5	464.6	293.6	6.3	97.1	105.3	229.6	1820.0	0.0
12	Taro	Ramiola	2	44.697°	10.094°	15.07.18	130	26.0	8.43	1403.7	56.2	565.3	529.5	6.6	136.5	144.4	242.7	1480.0	40.3
13	Baganza	Calestano	1	44.606°	10.123°	21.03.18	385	4.0	8.46	1881.2	33.4	423.4	312.2	12.7	105.4	99.4	220.9	1920.0	0.0
13	Baganza	Calestano	2	44.605°	10.120°	15.07.18	380	25.6	8.39	1253.1	42.1	504.1	681.0	12.9	123.6	253.7	338.0	1490.0	28.2
14	Parma	Pastorello	1	44.569°	10.237°	15.07.18	321	23.8	8.47	1315.0	41.0	429.5	694.2	8.8	81.3	185.1	315.3	1435.0	17.5
15	Enza	San Polo d'Enza	1	44.627°	10.413°	15.07.18	146	22.9	8.39	1473.5	58.9	560.6	868.2	8.9	88.6	235.4	434.5	1235.0	8.6
16	Secchia	Sassuolo	1	44.543°	10.767°	15.07.18	105	25.7	8.24	3944.4	99.9	875.3	10173.2	25.1	76.3	6070.4	3311.5	1100.0	0.0
17	Panaro	Marano sul Panaro	1	44.420°	10.925°	15.07.18	161	24.2	8.68	1362.2	54.6	461.6	589.1	5.1	80.0	211.6	282.6	1300.0	16.5
18	Reno	Marzabotto	1	44.338°	11.213°	01.05.17	126	15.1	8.79	1182.6	27.1	326.1	425.3	3.4	35.9	166.6	245.2	1408.7	12.9
18	Reno	Scuola	1	44.362°	11.257°	03.05.17	107	17.4	8.46	1632.1	54.1	483.3	1063.5	7.7	114.5	476.2	525.5	1698.5	8.3
18	Reno	Sibano	1	44.317°	11.185°	05.05.17	145	13.8	8.46	1147.5	63.6	308.1	393.0	3.1	45.8	154.8	204.6	1448.7	8.3
18	Reno	Lentula	1	44.079°	11.051°	05.05.17	584	11.2	8.31	865.4	22.8	203.3	129.6	1.7	108.1	581.5	685.4	1109.0	5.3
18	Reno	Castello di Sambuca	1	44.104°	10.998°	05.05.17	533	11.4	8.25	871.6	91.9	220.7	156.7	1.8	223.5	80.1	126.7	1049.1	10.5
18	Reno	Poretta Terme	1	44.100°	10.962°	04.05.17	483	10.1	8.37	1054.8	16.8	240.8	147.6	2.1	84.5	55.0	119.5	1149.0	26.1
18	Reno	Limentrella di Treppio	1	44.085°	11.044°	05.05.17	518	10.5	8.34	1030.0	97.7	297.2	112.5	1.9	249.5	50.4	115.7	1198.9	9.7
19	Senio	Casola Valsenio	1	44.227°	11.632°	15.07.18	155	23.2	8.57	1424.7	85.1	1221.9	1345.1	7.9	117.5	362.7	617.2	2050.0	29.0
20	Lamone	Biforco	1	44.065°	11.601°	15.07.18	326	18.7	8.57	1468.2	55.4	860.8	743.0	9.0	129.7	169.6	353.2	1835.0	15.7
21	Montone	Davadola	1	44.121°	11.885°	15.07.18	123	21.4	8.43	1429.5	80.4	954.5	1168.9	10.0	109.1	306.0	663.5	1680.0	29.5
21	Montone	San Benedetto	1	43.982°	11.689°	15.07.18	530	16.0	8.59	975.2	47.2	418.0	236.9	4.4	78.4	95.3	178.6	1180.0	42.2

Table S2. *Major dissolved ion concentrations and sampling location information.*

Catchment Number	Catchment Name	Locality	Sample Number	Latitude	Longitude	Bedrock Composition Correction	Date (dd.mm.yy)	Saturation Index	Corrected $[Ca^{2+}]$ (μmol/L)	Corrected $[Ca^{2+}]$ Error (μmol/L)	γ	(1)
1	Bisenzio	Vaiano	1	43.926°	11.127°	ND[†]	15 07 2018	1.35	ND[†]	ND[†]	ND[†]	ND[†]
2	Lima[#]	Cutigliano	1	43.999°	10.554°	Macigno-Cervarola	15 07 2018	0.69	3357.3	221.7	0.35	0.02
2	Lima[#]	Borgo a Mozzano	1	44.099°	10.752°	Macigno-Cervarola*	4 05 2017	-0.75	ND*	ND*	1.00	0.00
4	Serchio[#]	Filicaia	1	44.137°	10.374°	Macigno-Cervarola	15 07 2018	1	4055.7	261.0	0.41	0.02
5	Magra	Aulla	1	44.187°	9.926°	External Ligurian*	20 03 2018	0.01	ND*	ND*	1	0
6	Vara[#]	Aulla	1	44.190°	9.858°	Internal Ligurian*	20 03 2018	-0.78	ND*	ND*	1	0
6	Vara[#]	Piana Battolla	2	44.192°	9.858°	Internal Ligurian*	15 07 2018	0.69	ND*	ND*	1	0
7	Entella[#]	Piana Battolla	1	44.351°	9.362°	Internal Ligurian*	20 03 2018	-0.46	ND*	ND*	1	0
7	Entella[#]	Carasco	2	44.351°	9.362°	Internal Ligurian*	15 07 2018	0.33	ND*	ND*	1	0
8	Scrivia	Carasco	1	44.719°	8.860°	External Ligurian	18 03 2018	0.55	11531.7	610.1	0.13	0.01
9	Staffora	Serravalle Scrivia	1	44.893°	9.057°	External Ligurian	15 07 2018	0.6	15842.7	1044.4	0.09	0.01
10	Trebbia[#]	Godiasco	1	44.908°	9.590°	External Ligurian	22 03 2018	0.33	8706.3	480.7	0.16	0.01
10	Trebbia[#]	Rivergaro	2	44.909°	9.589°	External Ligurian*	15 07 2018	0.01	ND*	ND*	1	0
11	Nure[#]	Rivergaro	1	44.828°	9.617°	External Ligurian	15 07 2018	0.68	9857.5	870.1	0.12	0.01
11	Nure[#]	Vigolzone	1	44.882°	9.653°	External Ligurian	21 03 2018	0.46	15632.8	600.6	0.15	0.01
12	Taro[#]	Lugherzano	1	44.698°	10.093°	External Ligurian	21 03 2018	0.58	11140.0	566.9	0.13	0.01
12	Taro[#]	Ramiola	2	44.697°	10.094°	External Ligurian	15 07 2018	0.74	8923.1	585.4	0.16	0.01
13	Baganza[#]	Ramiola	2	44.605°	10.120°	External Ligurian	15 07 2018	0.65	15538.0	1075.0	0.08	0.01
13	Baganza[#]	Calestano	1	44.606°	10.123°	External Ligurian	21 03 2018	0.67	19210.0	1118.5	0.10	0.00
14	Parma[#]	Calestano	1	44.569°	10.237°	External Ligurian	15 07 2018	0.71	12629.7	819.3	0.10	0.01
15	Enza[#]	Pastorello	1	44.627°	10.413°	External Ligurian	15 07 2018	0.59	10675.5	836.3	0.14	0.01
17	Panaro	San Polo d'Enza	1	44.420°	10.925°	Macigno-Cervarola	15 07 2018	0.9	4503.3	361.7	0.30	0.02
18	Reno	Sassuolo	1	44.338°	11.213°	Macigno-Cervarola	1 05 2017	0.86	2200.3	150.3	0.54	0.03
18	Reno	Marano sul Panaro	1	44.362°	11.257°	Macigno-Cervarola	3 05 2017	0.76	5064.3	353.6	0.32	0.02
18	Reno	Marzabotto	1	44.317°	11.185°	Macigno-Cervarola	5 05 2017	0.51	1964.4	132.0	0.58	0.04
18	Reno	Scuola	1	44.079°	11.051°	Macigno-Cervarola	5 05 2017	0.09	1110.6	55.8	0.78	0.03
18	Reno[#]	Sibano	1	44.100°	10.962°	Macigno-Cervarola	4 05 2017	0.24	1402.8	85.6	0.75	0.04
18	Reno[#]	Lentula	1	44.085°	11.044°	Macigno-Cervarola	5 05 2017	0.23	1286.3	52.0	0.80	0.02
18	Reno[#]	Castello di Sambuca	1	44.104°	10.998°	Macigno-Cervarola	5 05 2017	0.03	1181.4	75.7	0.74	0.04
18	Reno[#]	Poretta Terme	1	44.183°	10.971°	Macigno-Cervarola	5 05 2017	0.91	2066.5	62.0	0.58	0.03
19	Senio[#]	Limentrella di Treppio	1	44.227°	11.632°	Marnoso Arenacea	15 07 2018	0.95	5553.9	336.2	0.26	0.01
20	Lamone[#]	Casola Valsenio	1	44.169°	11.688°	Marnoso Arenacea	15 07 2018	0.79	5670.3	306.0	0.25	0.01
20	Lamone[#]	Biforco	1	44.065°	11.601°	Marnoso Arenacea	15 07 2018	0.87	6775.2	345.1	0.22	0.01
21	Montone[#]	Davadola	1	44.121°	11.885°	Marnoso Arenacea	15 07 2018	0.71	7392.0	394.1	0.19	0.01
21	Montone[#]	San Benedetto	1	43.982°	11.689°	Marnoso Arenacea	15 07 2018	0.52	3385.4	167.5	0.29	0.01

[#]Samples used to constrain water chemistry mixing lines.
*Samples under or at saturation for which secondary calcite correction was not performed.
[†]Polluted sample for which additional analyses were not performed.
ND Values were not determined for these samples.

Table S3. *Saturation Index and results for secondary calcite precipitation correction.*

Catchment Name	Latitude	Longitude	Catchment Number	Sampling Date	[Ca^{2+}] lost to secondary precipitation (μmol/L)	Secondary Carbonate Flux (t/km^2/yr)	Percent of Total Denudation Flux
Baganza	44.6045°	10.1202°	13	15 07 2018	14284.9 ± 1075.7	1016.9 ± 76.6	140
Baganza	44.6061°	10.1226°	13	21 03 2018	17328.8 ± 1119.9	1233.6 ± 79.7	170
Entella	44.3509°	9.3619°	7	20 03 2018	0	0.0	0
Entella	44.3513°	9.3618°	7	15 07 2018	0	0.0	0
Enza	44.6267°	10.4133°	15	15 07 2018	9202.0 ± 837.4	895.3 ± 81.5	68
Lamone	44.0651°	11.6009°	20	15 07 2018	5307.0 ± 347.9	356.5 ± 23.4	43
Lima	43.9993°	10.5538°	2	15 07 2018	2172.8 ± 196.3	267.2 ± 24.1	53
Magra	44.1869°	9.9256°	5	20 03 2018	0	0.0 ± 0.0	0
Montone	44.1210°	11.8853°	21	15 07 2018	5962.5 ± 396.5	193.4 ± 12.9	13
Nure	44.82832°	9.6173°	11	15 07 2018	8414.6 ± 602.1	656.6 ± 47.0	62
Nure	44.8816°	9.6532°	11	21 03 2018	13827.0 ± 871.7	1078.9 ± 68.0	102
Panaro	44.41981°	10.9245°	17	4 07 2017	3141.1 ± 364.0	246.4 ± 28.6	31
Parma	44.5688°	10.23709°	14	15 07 2018	11314.6 ± 820.2	1144.7 ± 83.0	100
Reno	44.3380°	11.2125°	18	1 05 2017	1017.6 ± 133.6	68.3 ± 9.0	4
Reno	44.3622°	11.2573°	18	3 05 2017	3432.3 ± 299.1	230.3 ± 20.1	10
Scrivia	44.71943°	8.8602°	8	18 03 2018	9986.6 ± 611.8	583.5 ± 35.7	82
Senio	44.2266°	11.6324°	19	15 07 2018	4129.2 ± 338.9	217.2 ± 17.8	17
Serchio Filicaia	44.1374°	10.3741°	4	15 07 2018	2372.8 ± 236.3	135.0 ± 13.4	26
Taro	44.6976°	10.0934°	12	21 03 2018	9643.1 ± 568.7	813.7 ± 48.0	51
Taro	44.6975°	10.0936°	12	15 07 2018	7519.4 ± 587.0	634.5 ± 49.5	40
Trebbia	44.9081°	9.5897°	10	22 03 2018	7306.3 ± 482.5	603.0 ± 39.8	51
Trebbia	44.90890°	9.5893°	10	15 07 2018	0	0.0	0
Vara	44.1897°	9.8578°	6	20 03 2018	0	0.0	0
Vara	44.1919°	9.8584°	6	15 07 2018	0	0.0	0

Table S4. *Secondary carbonate fluxes and comparison with total denudation fluxes.*